ANL-HEP-CP-94-79
February 1, 2008

SCALE-INVARIANT LIPATOV KERNELS FROM t-CHANNEL UNITARITY

Claudio Corianò and Alan R. White *
High Energy Physics Division, Argonne National Laboratory, Argonne, IL 60439.

Abstract

The Lipatov equation can regarded as a reggeon Bethe-Salpeter equation in which higher-order reggeon interactions give higher-order kernels. Infra-red singular contributions in a general kernel are produced by t-channel nonsense states and the allowed kinematic forms are determined by unitarity. Ward identity and infra-red finiteness gauge invariance constraints then determine the corresponding scale-invariant part of a general higher-order kernel.

Presented at the Summer Institute on QCD, Gran Sasso (Aug 29 - Sept 11), the XXIV International Symposium on Multiparticle Dynamics, Vietri sul Mare (Sept 12-19), and the 2nd Workshop on Small-x and Diffractive Physics at the Tevatron, Fermilab (Sept 22-24).

*Work supported by the U.S. Department of Energy, Division of High Energy Physics, Contract W-31-109-ENG-38

1. INTRODUCTION

The small-x behavior of parton disributions has been the cause of much excitement. In particular, the "BFKL Pomeron"[1], i.e.

$$F_2(x,q^2) \ \sim \ x^{1-\alpha_0} \ \sim \ x^{-\frac{1}{2}} \tag{1}$$

may have been seen at HERA. This behavior is obtained by solving the Lipatov equation[1], written as an evolution equation for parton distributions, i.e.

$$\frac{\partial}{\partial(ln1/x)}F(x,k^2) \ = \ \tilde{F}(x,k^2) \ + \ \frac{1}{(2\pi)^3}\int \frac{d^2k'}{(k')^4} \ K(k,k')F(x,(k')^2) \tag{2}$$

where $K(k,q) \ = \ K^{(2)}_{2,2}(k,-k,q,-q)$ and $K^{(2)}_{2,2}$ is the full $O(g^2)$ Lipatov kernel defined below. To obtain non-leading corrections to the $O(g^2)$ kernel (which determine the crucial corrections to α_0) very complicated non-leading log Regge limit calculations are required. Can general Regge theory help?

Our answer is, of course, yes and our purpose in this talk is to show that the "scale-invariant" part of the $O(g^{2N})$ kernel, in which the gauge coupling does not run and there is no transverse momentum scale, is actually determined by the combination of Regge theory with gauge invariance. That is by the combination of multiparticle t-channel unitarity, continued in the j-plane[2], with Ward identity and infra-red finiteness constraints. We will outline a different, but closely related, method to that given in [3] for the explicit construction of higher-order kernels. Our methods are t-channel based and distint from the application of s-channel unitarity used by Bartels[4] to obtain higher-order results, although our results do overlap.

2. REGGEON FORMALISM

To introduce reggeon language we rewrite the Lipatov equation as a "reggeon Bethe-Salpeter equation". In effect we work backwards historically. We first extend (2) to the non-forward direction, then transform to ω - space (where ω is conjugate to $ln \ \frac{1}{x}$), giving

$$\omega F(\omega,k,q-k) \ = \ \tilde{F} \ + \ \frac{1}{(2\pi)^3}\int \frac{d^2k'}{(k')^2(k'-q)^2} \ K(k,k',q)F(\omega,k',q-k') \tag{3}$$

where $K(k,k',q) \;=\; K^{(2)}_{2,2}(k,q-k,k',q-k')$ now contains three kinematic forms i.e.

$$\frac{2}{3g^2}K^{(2)}_{2,2}(k_1,k_2,k_3,k_4) \qquad \equiv \qquad K_1 \;+\; K_2 \;+K_3 \qquad \equiv \qquad \sum_{1<->2}$$
$$\left(\frac{1}{2}(2\pi)^3 k_1^2 J_1(k_1^2) k_2^2\Big(k_3^2\delta^2(k_2-k_4)+k_4^2\delta^2(k_2-k_3)\Big) - \frac{k_1^2k_4^2 \;+\; k_2^2k_3^2}{(k_1-k_3)^2} - (k_1+k_2)^2\right) \tag{4}$$

and

$$J_1(q^2) \;=\; \frac{1}{(2\pi)^3}\int \frac{d^2k'}{(k')^2(k'-q)^2} \tag{5}$$

Moving the K_1 term to the left side of (3) and defining $G \;=\; \Gamma_2 F$ gives

$$G(\omega,k,q-k) \;=\; \tilde{G} + \frac{1}{(2\pi)^3}\int \frac{d^2k'}{(k')^2(k'-q)^2}\;\Gamma_2(\omega,k',q-k')\tilde{K}(k,k',q)G(\omega,k',q-k') \tag{6}$$

where $\Gamma_2(\omega,k_1,k_2) \;=\; [\omega - g^2k_1^2J_1(k_1^2) - g^2J_1(k_2^2)]^{-1}$, is a 2-reggeon propagator and

$$\tilde{K}(k,k',q) \;=\; K_2 \;+K_3 \;=\; \sum_{1<->2}\left(\frac{k_1^2k_4^2 \;+\; k_2^2k_3^2}{(k_1-k_3)^2} - (k_1+k_2)^2\right) \tag{7}$$

is a 2-2 reggeon interaction. That this interaction is singular is what makes it, at first sight, hard to understand from a Regge theory point of view.

If we write $\frac{1}{k^2} \sim \frac{1}{sin\pi\alpha' k^2}$ and arrange that α' scales out of the theory, then, apart from the singular interaction, (6) is a simple two-reggeon Bethe-Salpeter equation for odd-signature reggeons[4, 5]. In fact we can also include the K_1 term in the interaction and still write the reggeon equation (6) if we take $\Gamma_2(\omega,k_1,k_2) \;=\; [\omega - \alpha' k_1^2 - \alpha; k_2^2]^{-1}$, and ultimately take $\alpha' \to 0$. In this way we can also interpret (3) directly as a reggeon equation in which the interaction (the full $K^{(2)}_{2,2}$) then has two vital properties

- It is infra-red finite as an integral kernel i.e.

$$\int \frac{d^2k_1}{k_1^2}\frac{d^2k_2}{k_2^2}\delta^2(q-k_1-k_2)K^{(2)}_{2,2}(k_1,k_2,k_3,k_4) \qquad is \;\; finite \tag{8}$$

- It contains singularities (poles) but satisfies the Ward identity constraint

$$K^{(2)}_{2,2}(k_1,k_2,k_3,k_4) \;\; \to \;\; 0 \;\; , k_i \;\to\; 0 \;, i = \; 1,..,4 \tag{9}$$

These two properties determine the relative magnitude of the three kinematic forms K_1, K_2, and K_3. If we can derive their existence from a general Regge theory argument, as we do below, then the above properties determine the kernel uniquely.

It will be convenient to introduce a diagrammatic notation for transverse momentum integrals. A vertex with n incoming and m outgoing lines represents

$$(2\pi)^3\delta^2(\sum k_i \ - \sum k_i')(\sum k_i \ ) \tag{10}$$

and an n line intermediate state represents

$$(1/2\pi)^{3n} \int d^2k_1 ... d^2k_n \ / \ k_1^2 ... k_n^2. \tag{11}$$

We also define all kernels to include a factor $(2\pi)^3\delta^2(\sum k_i - \sum k_i')$, (they are then dimensionless and formally scale-invariant). We can then represent (4) as in Fig. 1, where the sum is over all distinct momentum permutations for all of the diagrams. We shall use these diagrams extensively in the following.

The higher-order corrections we want are evidently higher-order reggeon interactions. We will try to determine them by generalising the above discussion. As we have described in [3], generalisations of (8) and (9) are properties that should be satisfied by any (color zero) reggeon amplitude as a manifestation of gauge invariance. Our purpose now is to argue that the singular kinematic forms that can be present in a general reggeon interaction are actually determined by multiparticle t-channel unitarity continued in the ω or "j" - plane ($\omega = j - 1$). We shall then argue that (8) and (9) are sufficient to determine the scale-invariant part of a general interaction.

3. MULTIPARTICLE UNITARITY IN THE j - PLANE

It is well-known that multiparticle t-channel unitarity can be used to derive Regge cut discontinuities[2]. We can very briefly illustrate this as follows. Consider the four-particle intermediate state and insert Regge poles in the production amplitude as in Fig. 2. If we initially ignore the subtleties of signature we can write the relevant part of the j-plane continuation of this equation as a (double) helicity integral of the form

$$a_j - a_j^* = \int d\rho(t, t_1, t_2) \int \frac{dn_1 dn_2}{sin\pi n_1 sin\pi n_2 sin\pi(j - n_1 - n_2)} \frac{A^+ A^-}{(n_1 - \alpha_1)(n_2 - \alpha_2)} \tag{12}$$

where a_j is the elastic partial-wave amplitude, A^+ and A^- are production amplitude Regge pole residues and $\alpha_i \equiv \alpha(t_i), i = 1, 2$. When the Regge poles at $n_1 = \alpha_1$ and

$n_2 = \alpha_2$ combine with the "nonsense" pole at $j = n_1 - n_2 - 1$ to pinch the n_1 and n_2 integration contours in (12) we obtain

$$\int \frac{d\rho}{(j - \alpha_1 - \alpha_2)} \frac{A^+ A^-}{(sin\pi\alpha_1)(sin\pi\alpha_2)} \tag{13}$$

which produces a Regge cut (at $j = 2\alpha(\frac{t}{4}) - 1$), **provided** there is no "nonsense zero" in A. The requirement of no zero actually leads to the Regge cut appearing only in the even signature partial-wave amplitude.

The gluon reggeon (with $\alpha' \neq 0$) is present in the odd signature amplitude. In this amplitude the nonsense pole and the Regge poles in (12) combine to give

$$sin\pi j \int d\rho \frac{A^+ A^-}{(sin\pi\alpha_1)(sin\pi\alpha_2)} \tag{14}$$

where the $sin\pi j$ factor can be understood as originating from the nonsense zero. If we now insert $a_j \sim \frac{1}{(j-\alpha)}$ for $j - 1 \sim q^2 \to 0$ then (14) gives

$$\alpha(q^2) - 1 \ \sim \ q^2 \int \frac{d\rho}{sin\pi\alpha_1 sin\pi\alpha_2} \ \sim \ q^2 \int \frac{d^2k}{k^2(q-k)^2} \tag{15}$$

where now the q^2 factor providing the "reggeization" arises from the nonsense zero. We see that reggeization is explicitly due to the contribution of reggeon nonsense states.

If we move on to the six-particle intermediate state in the unitarity equation we find that the three reggeon nonsense states give singular terms in the 2-2 reggeon interaction i.e. the 2-2 Lipatov kernel. We will not give the details here (they will be given in a future publication). Instead we represent the construction as in Fig. 3. Clearly, if we add a constant 2-2 reggeon interaction, we generate the full set of transverse momentum diagrams for the Lipatov kernel. If we impose the properties (8) and (9) above we then **determine the full kernel from three-reggeon nonsense states without calculating a single Feynman diagram.**

In leading-order higher multiparticle nonsense states give **either** multi-reggeon cuts, **or** singularities of reggeon interactions i.e. **singular terms in higher-order kernels**. Note, however, that we can also apply the odd-signature analysis of (14) and (15) to the even signature channel contribution given by the non-leading behaviour of the partial-waves at the nonsense pole. This implies that even signature states will give nonsense-state contributions to reggeon interactions as a non-leading effect.

4. THE $O(g^4)$ KERNELS

The main contribution to the $O(g^4)$ 2-2 kernel is from the four-particle nonsense state, which we analyse via eight-particle unitarity. We consider all couplings of two reggeons to the nonsense states involved and combine them in all possible ways, as in Fig. 4. This gives the set of transverse momentum diagrams that can be generated. Putting nonsense zeroes for the vertices and imposing generalisations of (8) and (9) then gives $K_n^{(4)}$ uniquely. The diagrammatic representation of is given in Fig. 5. The full $O(g^4)$ kernel also contains a contribution from $(K_{2,2}^{(2)})^2$, where this kernel is defined as illustrated in Fig. 6. This contribution was not considered in [3]. It is important, in particular, because diagrams appear which are of the same form as the first diagrams (i.e. the disconnected bubbles) appearing in the four-particle nonsense state contribution above. These diagrams can not be associated with the reggeization of either of the interacting reggeons. This implies they have no Regge theory interpretation and must cancel. As a result the full $O(g^4)$ 2-2 kernel is determined to be

$$K_{2,2}^{(4)} \;=\; (K_n^{(4)} \;-\; K_{2,2}^{(2)})^2 \tag{16}$$

Using the above rules for diagrams gives the various contributions in the form given in [3].

We can also consider (N-M) reggeon interactions. At $O(g^4)$ the (2-4) interaction appears and the relevant nonsense states are shown in Fig. 7. Once again the gauge invariance constraints analagous to (8) and (9) uniquely determine the coefficients of the distinct transverse momentum diagrams. The result for $K_{2,4}^{(4)}$ is the (completely symmetrized) sum shown in Fig. 8. A complete expression for $K_{2,4}^{(4)}$ can be found in [3]. It is closely related to the kernel that appears in deep-inelastic high-mass diffraction[6].

5. CONSTRUCTION RULES FOR GENERAL HIGHER-ORDER KERNELS

From the above discussion it is clear that we can similarly construct a general high-order arbitrary (N-M) kernel. The leading contribution to $K_{2,2}^{(2N)}$ is from the (N+2) particle state. We draw all possible point couplings and combine them to form a full set of transverse momentum diagrams as in Fig. 9.We also have to add all posible products of lower-order kernels i.e.

$$(K^{(2)})^N \;+\; K^{(2)}\; K^{(4)}(K^{(2)})^{N-3} \;+\; ... \tag{17}$$

The cancellation of all disconnected diagrams that can not be interpreted in terms of reggeization will produce a large number of constraints and we anticipate that the collection of of Ward identity and infra-red finiteness constraints associated with a wide range of distinct kinematic forms will determine a unique scale-invariant kernel.

As a further example the contribution of the five-particle nonsense states to the $O(g^6)$ kernel is the symmetrized sum of diagrams (with coefficients that we have not determined) shown in Fig. 10. We also anticipate that kernels for general colored channels can be obtained by determining the appropriate color factor for each term relative to the color zero channel.

6. SCALE DEPENDENCE

From the construction it is, of course, clear that we will always obtain kernels that are (transverse momentum) scale-invariant. It is possible that these kernels have a fundamental relationship to the massless Regge region S-matrix. They may also be conformally invariant[1] (this is being studied). However, for physical applications we must input a scale. The simplest possibility, which we are not interested in here, is that the gluon becomes massive and this mass is added to all the transverse momentum propagators. Our interest is to input the off-shell renormalisation scale of QCD so that the evolution of the coupling, i.e. $g^2/4\pi \to \alpha_s(Q^2)$ somehow enters the formalism. This is non-trivial since we can expect that all the possible transverse momentum scales in a diagram will be involved in the scale-breaking.

Fadin and Lipatov have already calculated[7] the full trajectory function (that is the disconnected piece) in the next-to-leading log approximation in which we expect the $O(\alpha_s^2)$ kernel to appear. In addition to the off-shell renormalization effects, they find that the leading-log lns factors arise from $ln[s/k_\perp^2]$ where the $k_\perp$ may be, essentially, any internal transverse momentum. As a result the diagrams we have constructed contribute also with additional internal logarithm factors, as illustrated in Fig. 11.The important feature from our perspective is, however, that the diagram structure we have anticipated is what is found. This encourages us to try to determine the analagous logarithms that will occur as scale-breaking is introduced in the remainder of the kernel. It appears that we may be able to do this by an extension of the Ward identity plus infra-red finiteness analysis. As a "preliminary" result we note that the number of new diagrams do indeed seem to match the number of new conditions.

If we define new logarithmic vertex functions as in Fig. 12 then, as illustrated in Fig. 13, there are three kinematically distinct disconnected diagrams. There are also,

as illustrated in Fig. 14, nine further kinematically distinct new diagrams. For this set of nine diagrams there are four Ward identity and four infra-red finiteness constraints to determine the relative weights. There are three forms of divergence generated by further integration and so the relative weight of all the new disconnected pieces should be determined by overall infra-red finiteness.

As a matter of principle it is, perhaps, not clear that the full kernel should contain only (generalised) transverse momentum diagrams. Before we can adequately discuss this we need to carry out the analysis we have suggested. The component reggeon vertices already calculated by Fadin and Lipatov[8], that will go into their calculation of the full kernel, are certainly complicated. Nevertheless the reggeon interaction that provides the kernel is only a single partial-wave of the full 2-2 reggeon scattering amplitude. It is this partial-wave projection which combines with unitarity, as we have outlined, to determine that the infra-red behaviour of the kernel must be described by transverse momentum diagrams. If this can smoothly match with the asymptotic freedom of the coupling then our diagrammatic description, including scale-breaking, should be sufficient.

7. THE FUTURE

We have already studied the $O(g^4)$ scale-invariant 2-2 kernel in some detail and a paper describing various properties, including the leading eigenvalue, will appear shortly. Our hopes for the future include

- Determination of the complete $O(\alpha_s^2)$ kernel, as we have outlined.
- To understand how the scaling violations produced by the $\ln k_\perp^2$ factors combine with $\alpha_s(Q^2)$ to give simultaneous evolution in Q^2.
- Obtaining, perhaps, an all-orders "Reggeon Field Theory" describing simultaneouous evolution in $ln\frac{1}{x}$ and Q^2.
- Input (massless) quarks to study[9] the "soft Pomeron" and confinement at small $k_\perp$.

References

[1] L. N. Lipatov, in *Perturbative QCD*, ed. A. .H. Mueller (World Scientific, 1989); E. A. Kuraev, L. N. Lipatov, V. S. Fadin, *Sov. Phys. JETP* **45**, 199 (1977) ; Ya. Ya. Balitsky and L. N. Lipatov, *Sov. J. Nucl. Phys.* **28**, 822 (1978).

[2] A. R. White, *Int. J. Mod. Phys.* **A6**, 1859 (1990) and references therein.

[3] A. R. White, *Phys. Lett.* **B334**, 87 (1994).

[4] J. Bartels, *Nucl. Phys.* **B151**, 293 (1979), **B175**, 365 (1980), **DESY** *preprint*, DESY 91-074 (1991) and *Zeitsch. Phys.* **C60**, 471 (1993).

[5] J. B. Bronzan and R. L. Sugar, *Phys. Rev.* **D17**, 585 (1978).

[6] J. Bartels and M. Wusthoff, **DESY** *preprint*, DESY 94-016 (1994).

[7] V. S. Fadin, presentation at the Gran Sasso QCD Summer Institute (1994).

[8] V. S. Fadin and L. N. Lipatov, *Nucl. Phys.* **B406**, 259 (1993).

[9] A. R. White, *Int. J. Mod. Phys.* **A8**, 4755 (1993).

Figure Captions

Fig. 1 Diagrammatic representation of the $O(g^2)$ kernel.

Fig. 2 Regge pole contribution in the four-particle unitarity integral.

Fig. 3 The generation of elements of the $O(g^2)$ kernel by three reggeon nonsense states.

Fig. 4 The combination of nonsense couplings to give the transverse momentum diagrams generated by the four-particle nonsense state

Fig. 5 Diagrammatic representation of the four-particle $O(g^4)$ kernel

Fig. 6 The contribution to the $O(g^4)$ kernel from iteration of the two-particle nonsense state

Fig. 7 Nonsense states producing the $O(g^4)$ (2-4) kernel.

Fig. 8 Diagrammatic representation of $K_{2,4}^{(4)}$.

Fig. 9 The generation of transverse momentum diagrams for the $O(g^{2N})$ kernel.

Fig. 10 The $O(g^6)$ kernel generated by five-particle nonsense states.

Fig. 11 Additional logarithms in the trajectory function diagrams.

Fig. 12 New vertices - including logarithms.

Fig. 13 Disconnected (trajectory function) diagrams involving logarithmic vertices.

Fig. 14 The nine additional diagrams involving logarithmic vertices.

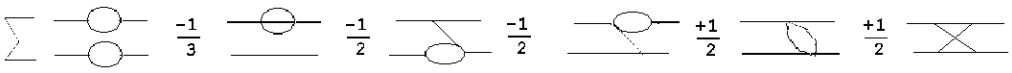

Fig. 1

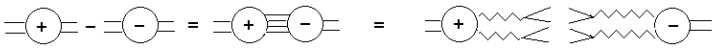

Fig. 2

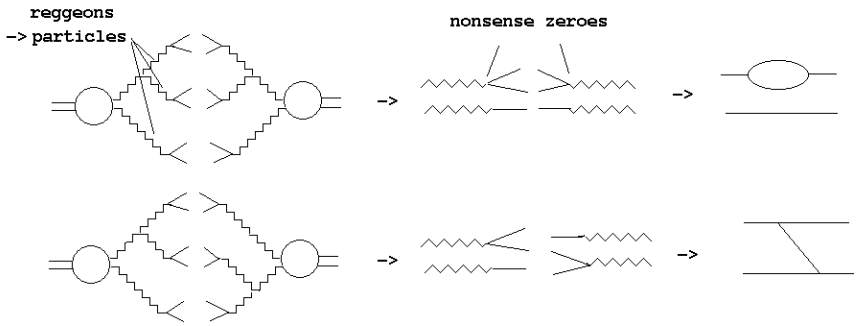

Fig. 3

Fig. 4

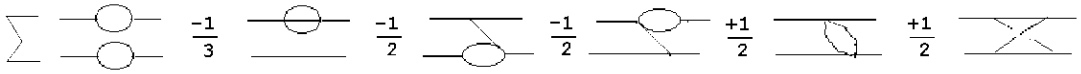

Fig. 5

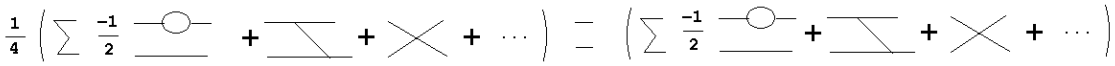

Fig. 6

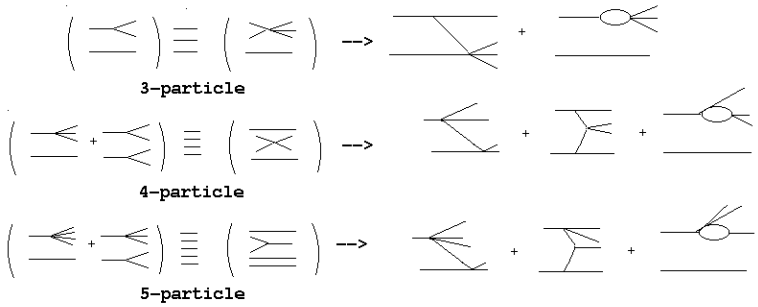

Fig. 7

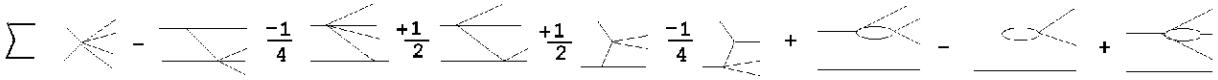

Fig. 8

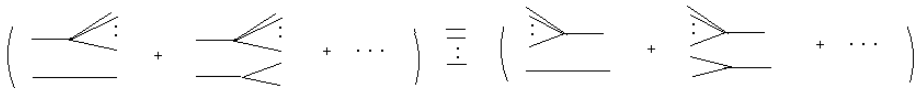

Fig. 9

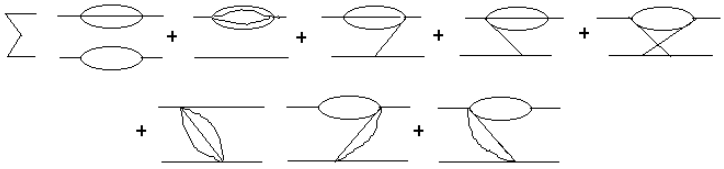

Fig. 10

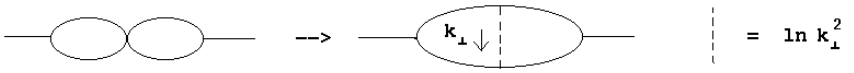

Fig. 11

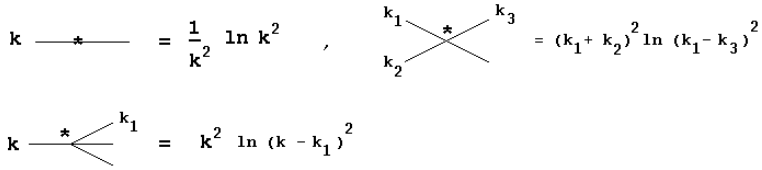

Fig. 12

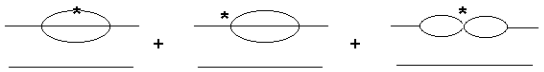

Fig. 13

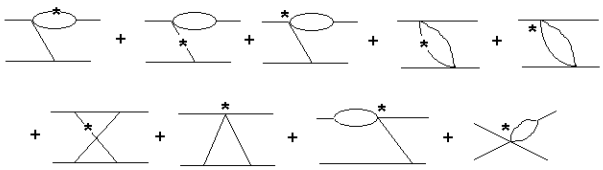

Fig. 14